Free Energy Perturbation Studies on Binding of the Inhibitor

5,6-dihydrobenzo[h]cinnolin-3(2H)one-2-acetic acid and its Methoxylated Analogs to Aldose Reductase

Giulio Rastelli,[‡*] Luca Costantino,[‡] Paola Vianello,[§] Daniela Barlocco[§]

[‡] Dipartimento di Scienze Farmaceutiche, Universita di Modena. Via Campi, 183. 41100 Modena (Italy)
[§] Istituto Chimico Farmaceutico e Tossicologico, Viale Abruzzi, 42. 20131 Milano (Italy)

Dedicated to Prof. G. Heinisch on the occasion of his 60th birthday

Abstract: Free energy perturbation simulations have been employed to rationalize the binding differences between a benzocinnolinone carboxylic acid inhibitor of aldose reductase and its methoxylated analogs in four selected substitution sites. The calculated free energy differences are in qualitative agreement with the experimental results. The balance between the cost for desolvation and the gain in enzyme binding correctly predicts and rationalizes the different inhibitory activities of each methoxylated compound. The implications for perturbations occurring at the interface between protein residues and water molecules present at the active site are discussed. © 1998 Elsevier Science Ltd. All rights reserved.

INTRODUCTION

Aldose reductase (ALR2; EC1.1.1.21) is an important enzyme in the development of degenerative complications of diabetes mellitus, through its ability to reduce excess D-glucose into D-sorbitol with the associated conversion of NADPH to NADP^{+}.[1] Several ALR2 inhibitors have been developed to date, most of which belong to the carboxylic acid and spirohydantoine classes of compounds.[2]

In a previous publication we reported that pyridazinone carboxylic acid compounds are potent and selective inhibitors of ALR2.[3] In that study, we also proposed the structure of the complex between ALR2 and one representative member (compound **1a**, R=H in Scheme 1) of this family of inhibitors using docking simulations followed by molecular mechanics and molecular dynamics calculations. In the complex, the carboxylate functional group, which is fundamental for inhibitory activity, hydrogen bonds to Tyr48, His110 and Trp111, and the carbonyl group hydrogen bonds to Cys298 (Figure 1). More recently, this complex was used as starting point for structure-based drug design, and a new analog with remarkably improved inhibitory activity was discovered.[4]

In the present work, we report free energy perturbation[5] (FEP) calculations on the binding of the 7-, 8-, 9- and 10-methoxylated analogs of compound **1a** (compounds **1b-e** in Scheme 1). These compounds have been synthesized and tested for their inhibition of ALR2.

The introduction of the methoxy substituent in these four substitution sites turned out to give substantial variations of inhibitory activity compared to the unsubstituted compound (Scheme 1). In the structure of the complex between ALR2 and the unsubstituted inhibitor **1a**,[3] these substitution sites were located towards the
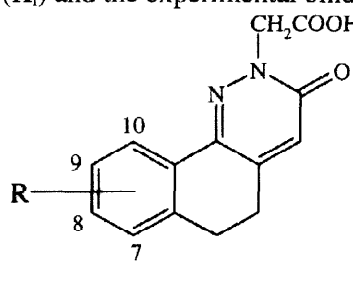
opening of the active site pocket, being at the interface between protein residues and solvent (Figure 1). We therefore decided to carry out free energy calculations on these methoxylated analogs both in water and in solvated aldose reductase, to see if we could reproduce the experimental findings and provide a rationale for the observed differences in inhibitory activities.

Figure 1: Selection of residues interacting with the unsubstituted benzocinnolinone carboxylic acid inhibitor **1a** in the structure of the complex with ALR2 (cross-eyed stereoview).[3] The hydrogen bonds between the carboxylate and Tyr48, His110 and Trp111, and those between the carbonyl and Cys298 are drawn as dashed lines. The water molecules are drawn as dots (oxygens). Hydrogens are omitted.
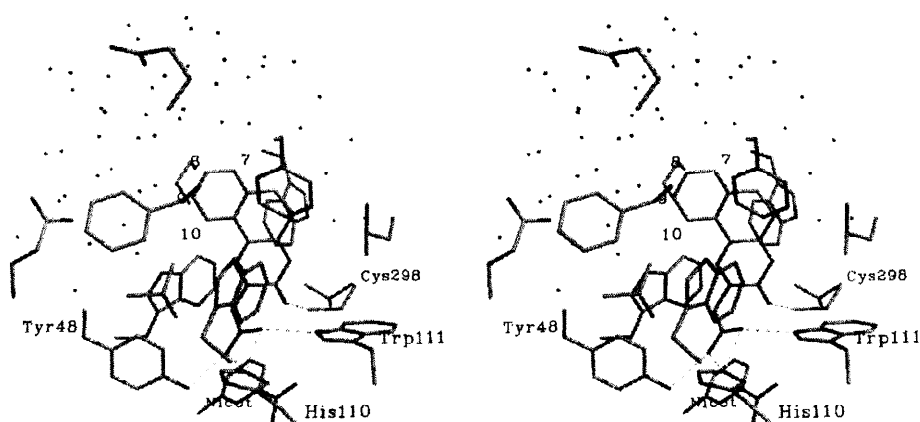
Scheme 1: Structures of the benzocinnolinone carboxilic acid inhibitors under investigation. The inhibition constants (K_i) and the experimental binding free energies (kcal/mol) to aldose reductase are reported.

		$K_i(\mu M)$	ΔG_{expt} [a]
1a	R=H	4.5	-7.34
1b	R=7-OCH₃	2.4	-7.71
1c	R=8-OCH3	3.7	-7.46
1d	R=9-OCH₃	15.6	-6.60
1e	R=10-OCH₃	63.0	-5.77
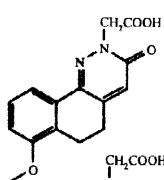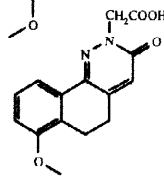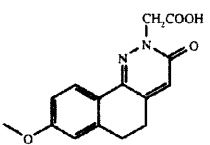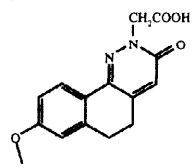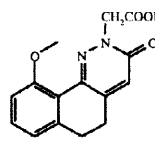
(a) Calculated using the formula $\Delta G° = RT\ln K_i$

RESULTS AND DISCUSSION

Compounds **1b-e** in Scheme 1 were synthesized as previously described for **1a**,[3] starting from the appropriate benzocinnolinone (**2**), in turn prepared from the required methoxytetralone (**3**). While the 5-, 6- and 7-substituted **3** were commercial products, the 8-methoxy derivative was synthesized from the known[6,7] 8-hydroxytetralone following standard procedures.
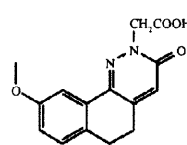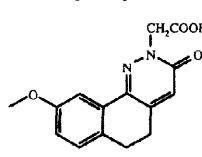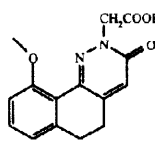
A preliminar analysis of the conformational features of the methoxy group in compounds **1b-e** was performed by optimizing their structures using AM1 and comparing their energies both in vacuo (AM1) and in water (AM1/SM2). With the exception of **1e**, two conformations of the methoxy substituent were found for each compound, both having the methoxyl coplanar with the aromatic ring but pointing in opposite directions (Scheme 2). As for the 7-methoxy derivative (**1b**), the conformation in which the methoxyl is directed towards the cinnolinone moiety (**1b''**) is 6.1 kcal/mol less stable in vacuo and 6.3 kcal/mol less stable in water with

Scheme 2: Relative stabilities (kcal/mol) in vacuo (AM1) and in water (AM1/SM2) of the two AM1-optimized conformations of each methoxylated compound.

Compound	ΔE^{AM1}	$\Delta E^{AM1/SM2}$
1b'	0	0
1b''	6.1	6.3
1c'	0	0
1c''	0.4	0.3
1d'	0	0
1d''	2.1	0.6
1e'	0	0
1e''	Not stable	

respect to 1b' (Scheme 2). Therefore, conformer 1b' is strongly preferred over 1b''. The two conformations of 1c (1c' and 1c'') have very similar energies both in vacuo and in water. Compound 1d is 2.1 kcal/mol more stable in conformation 1d' in vacuo, but the difference in energy with respect to 1d'' reduces to only 0.6 kcal/mol in water. Therefore, compounds 1c and 1d can reasonably adopt both conformations in water. The last compound, 1e, can only adopt conformation 1e'. In fact, no local minimum was even obtained for conformation 1e'', probably because of steric repulsion with the pyridazinone ring.

The most stable conformations of compounds **1b-e** were then selected for the FEP calculations presented below.

The FEP methodology was applied to calculate both solvation free energy differences and binding free energy differences between the analogs listed in Scheme 1. We used the thermodynamic perturbation method[8-10] to calculate the free energy differences.

The thermodynamic cycle relevant to this study is shown in Figure 2.

Figure 2: The thermodynamic cycle used to compute solvation (left) and protein binding (right) free energy differences. The horizontal free energies are experimentally determined, while the vertical free energies indicate mutations carried out by free energy perturbation simulations.

$$I_{(H)} + P \xrightarrow{\Delta G_1} I_{(H)}\text{-}P$$

$$\Delta G_{solv} \downarrow \qquad\qquad\qquad \downarrow \Delta G_{prot}$$

$$I_{(OCH_3)} + P \xrightarrow{\Delta G_2} I_{(OCH_3)}\text{-}P$$

$$\Delta\Delta G_{bind} = \Delta G_2 - \Delta G_1 = \Delta G_{prot} - \Delta G_{solv}$$
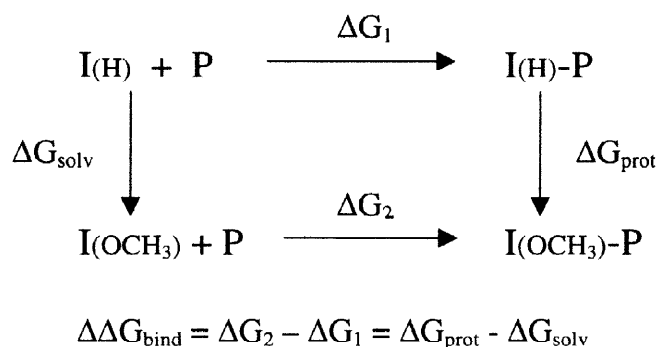
The free energies of binding to the protein, ΔG_1 and ΔG_2, of the two related inhibitors $I_{(H)}$ and $I_{(OCH_3)}$ are experimentally determined values, but they are difficult to calculate. ΔG_{solv} corresponds to mutating $I_{(H)}$ into $I_{(OCH_3)}$ in water, while ΔG_{prot} corresponds to changing $I_{(H)}$ into $I_{(OCH_3)}$ while bound to ALR2 in water. Since the thermodynamic cycle is closed and free energy is a state function, $\Delta\Delta G_{bind} = \Delta G_2 - \Delta G_1 = \Delta G_{prot} - \Delta G_{solv}$. While ΔG_{solv} and ΔG_{prot} represent physically unrealizable processes, these two simulations are computationally manageable. ΔG_1 and ΔG_2 have been calculated from the experimental inhibition constants of $I_{(H)}$ and $I_{(OCH_3)}$ (Scheme 1).

The free energy changes upon mutating the inhibitors are given in Table 1. Both forward (H→OCH3) and reverse (OCH3→H) simulations were performed, and the resulting ΔG values were averaged.

The free energy differences of solvation (ΔG_{solv}) for the perturbation H→OCH3 performed in the selected 7, 8, 9 and 10 positions of the reference benzocinnolinone carboxylic acid compound are negative, i.e. all the methoxylated analogs turn out to be more solvated than the parent unsubstituted inhibitor. This finding is consistent with the higher solvation free energy of anisole in previous benzene→anisole free energy perturbations.[11] The free energies of relative solvation calculated in the forward (H→OCH3) and reverse (OCH3→H) directions are fairly similar, therefore the hysteresys of these free energy calculations is very low. Moreover, the values of ΔG_{solv} calculated with free energy perturbation are in good agreement with the free energy differences of solvation calculated using the AM1/SM2 continuum model of solvation (Table 1).

The H→OCH3 free energy perturbations give significantly different relative free energies of solvation depending on the position of the methoxyl substituent. Position 10 gives the highest ΔG_{solv} (-2.90±0.09 kcal/mol), while position 7 gives the lowest ΔG_{solv} (-0.78±0.04 kcal/mol). Positions 8 and 9 give intermediate values (-1.81±0.02 kcal/mol and -1.00±0.07 kcal/mol, respectively).

Table 1: Calculated free energy differences (kcal/mol) in water and in solvated aldose reductase.

Perturbation	run	length(ps)	in Water		$\Delta G_{solv}^{AM1/SM2(c)}$	in Aldose Reductase		$\Delta\Delta G_{bind}^{(a)}$	$\Delta\Delta G_{expt}^{(b)}$
			ΔG_{solv}	$<\Delta G>_{solv}$		ΔG_{prot}	$<\Delta G>_{prot}$		
7H→7OCH₃	forward	200	-0.82±0.05	-0.78±0.04	-1.25	-1.53±0.03	-1.50±0.03	-0.72±0.05	-0.37
	reverse	200	0.74±0.07			1.47±0.04			
8H→8OCH₃	forward	200	-1.82±0.12	-1.81±0.02	-1.94	-1.92±0.03	-2.02±0.10	-0.21±0.10	-0.12
	reverse	200	1.79±0.17			2.12±0.18			
9H→9OCH₃	forward	200	-1.07±0.03	-1.00±0.07	-1.89	-1.97±0.21	-1.90±0.08	-0.90±0.11	0.74
	reverse	200	0.93±0.07			1.82±0.05			
	forward	400	-1.18±0.06			-1.20±0.09		-0.02±0.11	
10H→10OCH₃	forward	200	-2.81±0.08	-2.90±0.09	-2.99	-1.55±0.12	-1.31±0.24	1.59±0.26	1.57
	reverse	200	2.99±0.30			1.06±0.15			
7OCH₃→7H[d]									
electrostatic	forward	200	-0.14±0.02			0.21±0.03			
vdW	forward	400	0.62±0.08			0.79±0.03			
total			0.48±0.08			1.00±0.06		0.52±0.09	0.37[e]
9OCH₃→9H[d]									
electrostatic	forward	200	-0.06±0.01			-0.21±0.01			
vdW	forward	400	0.66±0.04			0.41±0.10			
total			0.60±0.04			0.20±0.11		-0.40±0.11	-0.74[e]

(a) $\Delta\Delta G_{bind} = <\Delta G>_{prot} - <\Delta G>_{solv}$ (b) Experimental free energy differences of binding referred to the unsubstituted (R=H) compound. (c) Solvation free energy differences according to the AM1/SM2 method. (d) Perturbation in the direction of the disappearance of the methoxy group using electrostatic decoupling. (e) These ΔG_{expt} are reported with opposite sign because the perturbation is run in the methoxy→hydrogen direction.

The free energy differences obtained from the same mutations into the solvated binding site of aldose reductase are also reported in Table 1. For the mutations in the direction H→OCH₃, negative values of ΔG_{prot} were obtained in all cases, as previously found for ΔG_{solv}. However, since the ΔG values from the protein and the water simulations are fairly different, their balance turn out to be determinant for the effective binding. According to the thermodynamic cycle shown in Figure 2, the averaged ΔG_{prot} and ΔG_{solv} values were subtracted to obtain $\Delta\Delta G_{bind}$ values. The resulting $\Delta\Delta G_{bind}$, also reported in Table 1, have been compared with the experimental free energy differences ($\Delta\Delta G_{expt}$).

The free energy simulations are able to qualitatively reproduce the experimental binding free energy differences between the methoxylated analog in question and the unsubstituted reference compound, with the exception of the 9OCH₃ analog that will be discussed later. In particular, the FEP simulations are able to reproduce the stronger binding of the 7-methoxy derivative: it is -0.78 kcal/mol more solvated than the unsubstituted compound, but it is -1.50 kcal/mol more stable when complexed by solvated aldose reductase, with a net gain in binding energy of –0.72 kcal/mol vs the experimental value of -0.37. The free energy results for the perturbation 8H→8OCH₃ are also in very good agreement with experiment ($\Delta\Delta G_{bind}$= -0.21 kcal/mol, $\Delta\Delta G_{expt}$= -0.12 kcal/mol). Interesting observations can be made comparing the 7H→7OCH₃ and 8H→8OCH₃ free energy results. ΔG_{prot} for the 8H→8OCH₃ perturbation is about 0.5 kcal/mol lower than the correspondent value of the 7H→7OCH₃ perturbation (-2.02 kcal/mol vs –1.5 kcal/mol, respectively). This indicates that the 8OCH₃ substituted compound interacts more favorably with the protein and water molecules of the active site with respect to 7OCH₃. However, the 8OCH₃ compound is penalized by a significantly higher free energy difference of solvation in water with respect to 7OCH₃ (ΔG_{solv} being –1.81 kcal/mol and –0.78 kcal/mol, respectively), with the net result that the 8OCH₃ inhibitor is predicted to be less active than the 7OCH₃ inhibitor in spite of its stronger binding to aldose reductase, in agreement with experiment.

The importance of the balance between ΔG_{prot} and ΔG_{solv} in determining the effective binding of the inhibitors is even more evident for the 10H→10OCH₃ perturbation. Free energy results correctly predict the much lower binding of the 10-methoxy derivative 1e ($\Delta\Delta G_{bind}$=1.59 kcal/mol vs $\Delta\Delta G_{expt}$=1.57 kcal/mol). Compared to 7OCH₃ and 8OCH₃, the 10OCH₃ compound combines the highest solvation free energy difference in water within the series (ΔG_{solv}=-2.90 kcal/mol) with the lowest free energy difference of binding to aldose reductase (ΔG_{prot}=-1.31 kcal/mol). Therefore, the large cost paid by desolvating the inhibitor offsets the modest gain in binding to solvated aldose reductase, resulting in a remarkably less active inhibitor.

The 9H→9OCH₃ perturbation performed using the 200ps molecular dynamics simulation predicts the 9-methoxy analog to be more active than the unsubstitued compound, in disagreement with the experimental result: $\Delta\Delta G_{bind}$ is -0.90 kcal/mol , while $\Delta\Delta G_{expt}$ is 0.74 kcal/mol. Although very good agreement was found in the other three cases, the large error in predicting the binding of the 9-methoxy compound (1.64 kcal/mol) led us to further investigations.

First of all, the final structures obtained at the end of the H→OCH₃ perturbations in aldose reductase were further subjected to 200ps of molecular dynamics (MD) using the methoxyl topologies, to see if significant changes exist between these structures and to gain insight into the conformation of the methoxy group during MD. At this end, structures were collected every 0.2ps and averaged at regular intervals. In addition, a monitoring of the dihedral angle determining the rotation of the methoxyl was also performed.

The structures of the complexes are reported in Figure 3. In all cases, the carboxylate substituent of the methoxylated compounds give strong hydrogen bonds with Tyr48, His110, Trp111, and the carbonyl substituent hydrogen bonds to Cys298, as previously shown for the parent unsubstituted compound 1a (Figure 1). As for compound 1b, only the lowest-energy conformation of the 7-methoxy substituent is sampled during MD (1b' in Scheme 2), and the 7-methoxy group is mainly exposed to water molecules of the active site (Figure 3). For compound 1c, MD samples both conformations of the 8-methoxy substituent, in agreement with the very similar energies of the two conformations (1c' and 1c'' in Scheme 2). Therefore, compound 1c is able to bind ALR2 by adopting both conformations, and their structures have been superimposed in Figure 3.

Figure 3: Final structures of the methoxylated compounds **1b–e** bound at the active site of ALR2 obtained after the H–OCH3 perturbations and further molecular dynamics calculations (stereoviews). For compounds **1c** and **1d**, the two structures corresponding to the different conformations of the methoxy substituent sampled during molecular dynamics have been superimposed.

1b
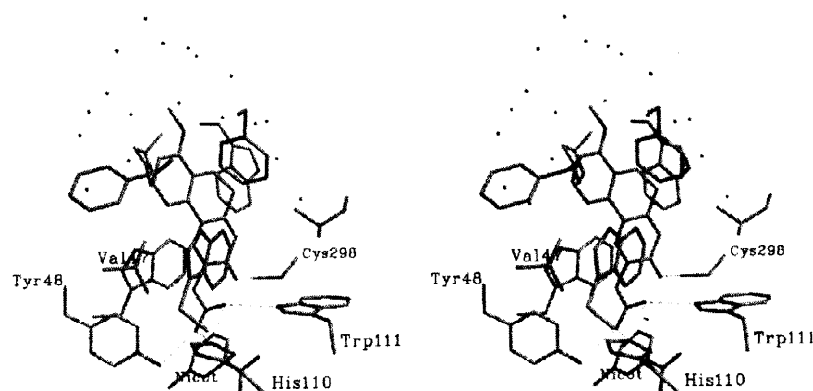
1c
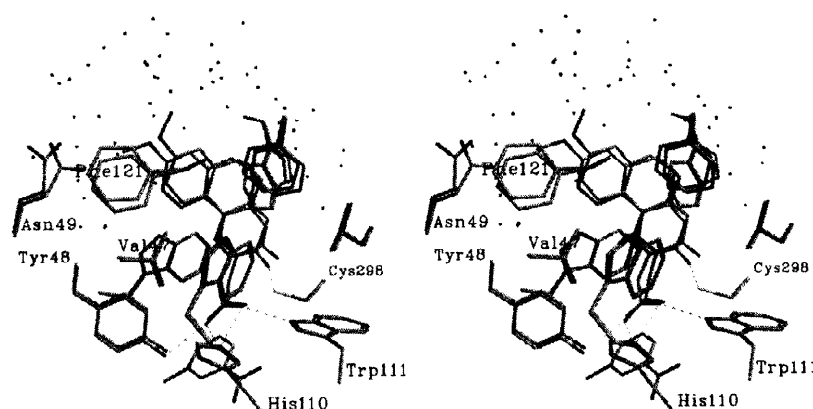
1d
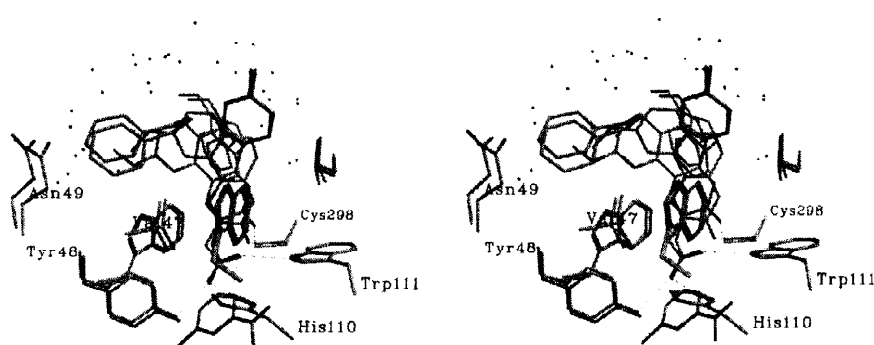
1e
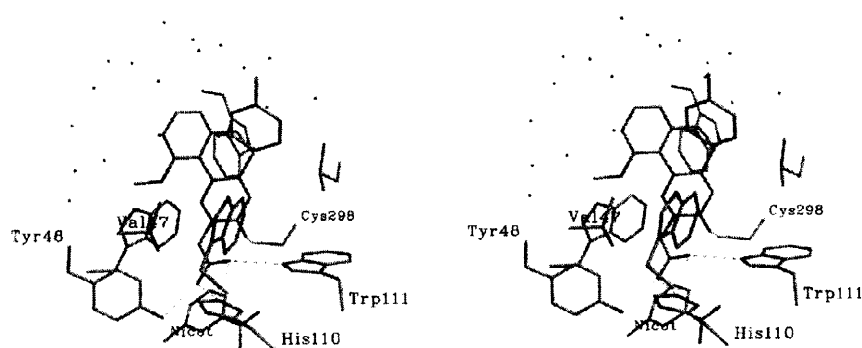
Worth of note is that the orientation of the inhibitor into the binding site is very similar in the two conformations, as evidenced by the fairly good overlap of the inhibitor structures in the superimposition. The situation is different for the 9-methoxy compound 1d. MD still samples both conformations of the methoxy group, in agreement with the AM1 data in Scheme 2, but the orientation of the inhibitor inside ALR2 is significantly different in the two conformations, as can be seen from the superimposition in Figure 3. Probably, the rotation of the 9-methoxy group determines steric conflicts with the Val47, Tyr48 and Trp20 side chains, so that the bulk inhibitor is displaced when the methoxyl is directed toward these residues. Finally, MD samples only one conformation of the 10-methoxy derivative 1e, again in accord with the AM1 results (1e', Scheme 2).

In conclusion, while 1b and 1e sample only one conformation of the methoxyl and give fairly stable averaged structures during MD, compounds 1c and 1d bind ALR2 in both conformations. Remarkably, while the orientation of the inhibitor 1c is almost identical in the two conformations, the orientation of 1d is significantly dependent upon the conformation adopted by the 9-methoxyl. This peculiar feature of the 9-methoxy derivative could explain the large error in predicting the free energy difference of binding to ALR2 of this compound. In fact, sampling of conformational states is particularly difficult in this case, and free energy results may have not converged. Even though 200ps simulations are generally short to conceivably sample the configurational space of complex systems, it is surprising that both forward (9H→9OCH$_3$) and reverse (9OCH$_3$→9H) perturbations in water and in aldose reductase give fairly similar free energy differences, resulting in a very low hysteresys. However, a small hysteresys is not, itself, sufficient to claim convergence. Therefore, in order to examine the convergence behaviour of these free energy results, we decided to perform twice as long simulations for this particular perturbation (400ps). The free energy difference of solvation from the 400ps simulation turns out very similar to that previously obtained from the 200ps simulation (-1.18 kcal/mol vs -1.00 kcal/mol, respectively). On the contrary, the free energy difference of binding to aldose reductase is significantly different, being -1.20 kcal/mol in the 400ps simulation and -1.90 kcal/mol in the 200ps simulation. The value of $\Delta\Delta G_{bind}$ obtained from the 400ps simulation is -0.02 kcal/mol (Table 1). While the error in predicting the experimental binding of the 9-methoxy compound is significantly reduced (from 1.64 kcal/mol to 0.76 kcal/mol in the 200ps and 400ps simulations, respectively), the agreement with experiment is still not completely satisfactory. Therefore, in order to see if we could reproduce the experimental value under different simulation conditions, we also choose to perform 'electrostatic decoupling' simulations,[12] i.e. to separate the electrostatic and van der Waals (vdW) contributions in two different and consecutive simulations. This method is particularly suited to perturbations that involve the appearance or the disappearance of large groups,[12] as is the case of the H→OCH$_3$ perturbations presented here. In general, water molecules and protein residues might get too close to the appearing or disappearing groups, causing an instability in the simulations. This problem can be particularly evident near the end points of the mutation when there are partial charges on atoms with very small vdW parameters.

Electrostatic decoupling simulations were performed for the 7OCH$_3$→7H perturbation first, in order to test the performance of the new method in a case in which $\Delta\Delta G_{bind}$ from the 200ps simulation agrees with experiment, and then performed for the 9OCH$_3$→9H perturbation. The electrostatic part was calculated from a 200ps simulation, and the vdW part, which is usually slower to converge, was done in 400ps.

The free energy results obtained for the 7OCH$_3$→7H and 9OCH$_3$→9H perturbations under these new conditions are included in Table 1. The opposite signs of $\Delta\Delta G_{expt}$ in these electrostatic decoupling calculations come from the fact that these perturbations must be run in the direction of the disappearing methoxy group (OCH$_3$→H). The $\Delta\Delta G_{bind}$ for the 7OCH$_3$→7H perturbation is in full agreement with the experimental result ($\Delta\Delta G_{bind}$ =0.52 kcal/mol, $\Delta\Delta G_{expt}$ =0.37 kcal/mol in the direction of the disappearing methoxy group). Noteworthy, this $\Delta\Delta G_{bind}$ value is even closer to experiment than the $\Delta\Delta G_{bind}$ obtained without electrostatic decoupling. As for the 9OCH$_3$→9H perturbation, the calculated $\Delta\Delta G_{bind}$ of -0.40 kcal/mol now closely reproduces the experimental $\Delta\Delta G_{expt}$ of -0.74 kcal/mol, with an error reduced to 0.34 kcal/mol. In conclusion,

the 400ps simulation for the 9H→9OCH$_3$ perturbation without electrostatic decoupling significantly reduces the error in predicting the $\Delta\Delta G_{bind}$, probably because of better sampling of conformational states with respect to the 200ps simulation, and the electrostatic decoupling simulation yields results even closer to experiment, probably because the separation between electrostatic and vdW contributions into two different 200ps and 400ps simulations further alleviates sampling difficulties.

By inspection of the structure of the complex between aldose reductase and the unsubstituted reference inhibitor **1a** (Figure 1) and of the methoxylated inhibitors **1b-e** (Figure 3), it is evident that, besides protein residues, there are a huge number of water molecules surrounding positions 7, 8, 9 and 10 of the inhibitor. Accordingly, since the perturbations occur at the interface between protein residues and solvent molecules of the active site, only partial desolvation is conceivably required to bind the methoxylated inhibitors. On interpretative grounds, the free energy perturbations presented in this work reflect the substitution of a pure water molecules environment (water simulations) with a mixed protein residues/water molecules environment (aldose reductase/water simulations). On the front of methodology, it is encouraging that we have been able to reproduce experimental free energies for perturbations that involve only a partial desolvation, since most FEP calculations that have been reported to date involve a complete desolvation of the perturbed group when binding to the host. As a whole, our results call attention to the possibility, for the future, to design new molecular substitutions specifically targeted at the interface between protein residues and water, and to quantitatively predict the associated differences in binding affinity.

CONCLUSIONS

We have presented free energy perturbation calculations of the binding of four methoxylated analogs of a previously discovered benzocinnolinone carboxylic acid inhibitor of aldose reductase. These calculations were undertaken to provide a rationale to the experimental inhibitory activities of these compounds, and to investigate whether FEP methodology was able to reproduce experimental results for hydrogen→methoxy perturbations that occur at the interface between protein residues and water molecules present in the active site.

The calculations were able to reproduce the correct rank order of activity of the methoxylated analogs under investigation. In particular, free energy results qualitatively reproduced the higher binding of the 7- and 8- methoxylated analogs, and the lower binding of the 9- and 10- methoxylated compounds with respect to the unsubstituted reference inhibitor. The balance between solvation free energies in water (the cost that the inhibitor must pay to desolvate before binding) and binding free energies to aldose reductase (the gain in free energy upon binding) correctly accounted for and provided an explanation to the experimental results. A peculiar feature of this study is that, since perturbations occur at the interface between protein residues and solvent of the active site, only partial desolvation is required to bind the inhibitors. The agreement between theory and experiment found in the simulations presented here is encouraging for future investigations of mutations that occur towards the opening of active site pockets of proteins and receptors.

EXPERIMENTAL SECTION

Computational Methods

The AMBER4.1[13] program was used for all molecular mechanics (MM), molecular dynamics (MD) and free energy perturbation (FEP) calculations. The all-atom force field by Cornell et al.[14] was used. During MD and FEP simulations, all bond lenghts were constrained using the SHAKE[15] algorithm, allowing a time step of 2.0 fs. Solute and solvent were coupled to a constant temperature heat bath with a coupling constant of 0.2 ps to maintain a temperature of 300K. A residue based cutoff of 10Å was employed. Pairlists were updated every 25 time steps. In FEP, the entire inhibitor was treated as the perturbed group. No intraperturbed group contributions to the free energy were calculated.

The starting coordinates for FEP calculations were taken from our previous model structure of the unsubstituted inhibitor (Scheme 1, R=H) bound in the active site of aldose reductase.[3] Counterions were placed around the charged residues at the surface of the enzyme in order to have a total charge of -1. The -1 charge was chosen so as to have the same net charge in the enzyme and in the water simulations (i.e. the negative charge of the dissociated carboxylate of the inhibitor). The oxidized form of NADPH (NADP+) was used in all simulations because inhibitors preferentially bind this form.[16] The parameters for NADP+ were set consistently with the Cornell et al force field; the parameters for the oxidized nicotinamide ring were taken from our previous simulations.[3] The atomic charges of the nicotinamide ring were recalculated with an electrostatic potential fit to a 6-31G* ab-initio wave function, followed by a standard RESP fit.[17,18] As regards the inhibitors, their structures were completely optimized using AM1, and charges were calculated with electrostatic potential fits to a 6-31G* ab-initio wave function, followed by RESP. The partial charges of the inhibitors are reported in Scheme 3.

Four independent perturbations were carried out starting from the model inhibitor (R=H) in Scheme 1. In order to set up the perturbation hydrogen→methoxy, dummy atoms were added to the 7, 8, 9, and 10 positions of the benzene terminal ring. These dummy atoms had the same bond parameters of a methoxy group, but zero charges and zero van der Waals parameters. The additional force constants for the bond and dihedral parameters terms of the methoxy group were taken from ref 11.

The active site of ALR2 containing the inhibitor and NADP+ was solvated with a spherical cap of 860 TIP3P[19] water molecules within 24Å of the center of mass of the inhibitor, and harmonic radial forces (1.5 kcal/mol Å²) were applied to these waters to avoid evaporation.

The energy minimization was performed by optimizing the water molecules first, keeping the rest of the system frozen. In addition, 10ps MD at 300K were performed on the water molecules only, in order to let the solvent equilibrate around the protein and the inhibitor. Then, energy minimization was continued by letting the inhibitor, NADP+ and all the protein residues within 10Å from the inhibitor free to move. The minimized structure was equilibrated with MD at 300K for 45ps. During the first 5ps of equilibration, a 5 kcal/mol restraint was applied on the inhibitor, and then it was removed.

The perturbations were carried out in a series of 50 windows with $\Delta\lambda=0.02$, with 1000 steps of equilibration and 1000 steps of data collection, summing up to a total simulation time of 200 ps for each run. Simulations were run both in the forward ($\lambda=1\rightarrow0$) and in the reverse ($\lambda=0\rightarrow1$) direction, with 10ps equilibration at $\lambda=0$ before running the reverse simulation.

For mutations in water, the inhibitor was placed at the center of a rectangular box of 1286 TIP3P water molecules. The system was equilibrated at 300K under periodic boundary conditions, using a minimization/equilibration simulation protocol similar to that above described. Then, mutations were performed as already described for aldose reductase.

Solvation free energy differences between the inhibitors were also calculated using the continuum solvation model AM1/SM2[20] incorporated into AMSOL[21]. The inhibitors were fully geometry optimized in water using AM1/SM2, and free energies of solvation were calculated on the optimized geometries.

Scheme 3: Partial charges of the inhibitors calculated using a RESP fit to 6-31G* wave functions.
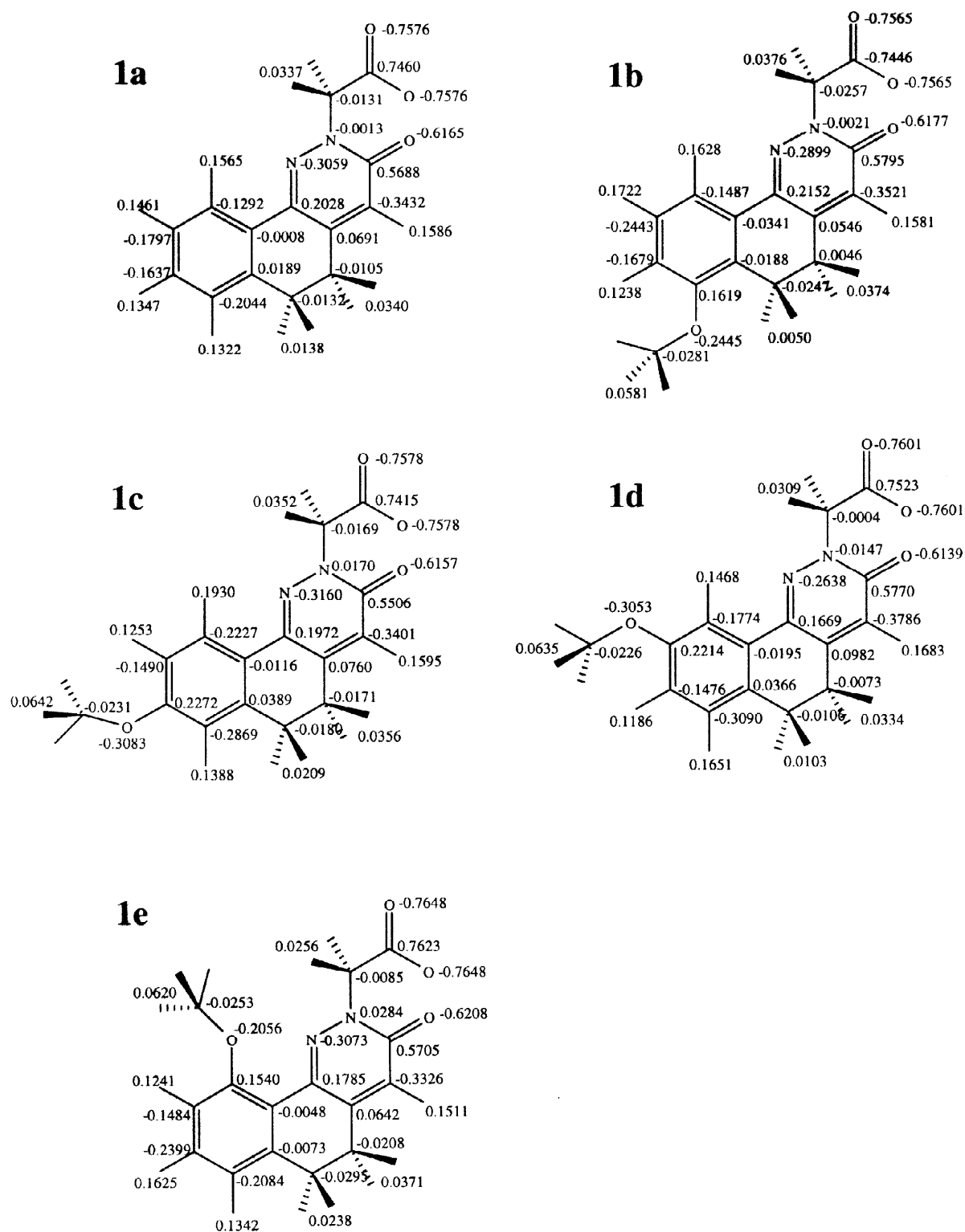
Since the 9H→9OCH$_3$ perturbation gave the poorest agreement between the calculated $\Delta\Delta G_{bind}$ and the experimental $\Delta\Delta G$ value, 400ps simulations in the forward direction were performed both in water and in aldose reductase for this particular case. Moreover, a different protocol was tried. We used 'electrostatic decoupling' to separate the total free energy difference into its electrostatic and van der Waals contributions.[12] For this type of perturbation, the 9OCH$_3$ topology had to be defined at $\lambda=1$ (initial state), and the perturbation run in the direction of the disappearing group (i.e. the 9OCH$_3$→9H direction). Each contribution was then calculated in separate simulations, both in water and in aldose reductase. The electrostatic part was calculated performing a 200ps perturbation, after which the van der Waals part was run in 400ps. Electrostatic decoupling simulations were performed for the 7OCH$_3$→7H perturbation first, in order to test the performance of the new method in a case in which $\Delta\Delta G_{bind}$ values are in agreement with experiment.

Calculations were performed on Silicon Graphics O2 workstations.

Chemistry

Melting points were determined on a Büchi 510 capillary melting points apparatus and are uncorrected. ^{1}H-NMR spectra were recorded on a Bruker AC200 spectrometer; chemical shifts are reported as δ (ppm). TLC on silica gel plates was used to check product purity. Silica gel 60 (Merck; 70-230 mesh) was used for column chromatography.

8-Methoxy-1-tetralone. To a solution of 8-hydroxy-1-tetralone[6,7] (0.3 g; 1.85 mol) in acetone (25 ml) potassium carbonate (0.41 g; 2.96 mmol) and dimethylsulfate (0.31 ml; 3.28 mmol) were added and the mixture refluxed for 62 h. After evaporation of the solvent, water (30 ml) was added and the mixture extracted with dichloromethane (3 x 15 ml). The collected organic fractions were dried over sodium sulfate, the solvent evaporated and the residue purified by silica gel chromatography, eluting with cyclohexane/ethyl acetate 7/3, to give 0.2 g (61.3 %) of the desired compound as an oil. ^{1}H NMR (CDCl$_3$) δ 2.0 (2H, m); 2.58 (2H, t, J=6.80 Hz); 2.90 (2H, t, J=6.66 Hz); 7.15 (3H, m).

General method for the synthesis of substituted-5,6-dihydrobenzo[h]cinnolin-3(2H)ones-2-acetic acids 1b-e. A mixture of the required benzocinnolinone 2 (0.01 mol), ethylbromoacetate (0.02 mol) and potassium carbonate (0.02 mol) in acetone (40 ml) was refluxed overnight. After cooling, the inorganic salts were filtered off, the solvent evaporated and the so formed esters hydrolyzed by stirring with sodium hydroxide (0.04 mol) in ethanol (40 ml) at rt for 2 h.

Inhibition of ALR2

The IC$_{50}$ values (the concentration of the inhibitor required to produce 50% inhibition of the enzyme-catalyzed reaction) were determined using the procedure described in reference 3. Since the inhibition constants (K_i) for some pyridazinone carboxylic acid inhibitors were determined under identical conditions in previous work,[3] the Cheng and Prusoff[22] equation was used to calculate the inhibition constants K_i from the IC$_{50}$ values of the methoxylated analogs here reported (see ref 23 as a recent application of this procedure). The K_i were then transformed into binding free energies by means of the equation $\Delta G^\circ=RTlnK_i$.

The experimental data are summarized in Table 2.

Table 2: Yields, melting points, spectroscopic data and inhibitory activities.

Compound	Yield	mp/°C	^{1}H NMR (DMSO-d_6)	IC$_{50}$ (μM)	K$_i$(μM)
1a$^{(a)}$				12.6	4.5
1b	70	255-257	2.9 (4H,s); 3.8 (3H,s); 4.8 (2H,s); 6.9 (1H,s); 7.1 (1H,q); 7.3 (1H,t); 7.6 (1H,q); 13.0 (1H,br.s)	6.7	2.4
1c	56	190-193	2.9 (4H,s); 3.8 (3H,s); 4.8 (2H,s); 6.9 (1H,s); 7.0 (1H,s); 7.9 (1H,m); 13.0 (1H,br.s)	10.3	3.7
1d	67	243-245	2.9 (4H,s); 3.8 (3H,s); 4.8 (2H,s); 6.9 (1H,s); 7.3 (1H,d); 7.5 (1H,d); 13.0 (1H,br.s)	43.6	15.6
1e	53	204-206	2.9 (4H,s); 3.8 (3H,s); 4.8 (2H,s); 6.9 (1H,s); 7.2 (3H,m); 13.0 (1H,br.s)	175	63.0

(a) reference 3. IC$_{50}$ of sorbinil is 3.04 μM.

REFERENCES

1) Tomlinson, D.R.; Stevens, E.J.; Diemel, L. *Trends Pharm. Sci.* **1994**, *15*, 293.

2) Costantino, L.; Rastelli, G.; Cignarella, G.; Vianello, P.; Barlocco, D. *Exp. Opin. Ther. Patents* **1997**, *7*, 1.

3) Costantino, L.; Rastelli, G.; Vescovini, K.; Cignarella, G.; Vianello, P.; Del Corso, A.; Cappiello, M.; Mura, U.; Barlocco, D. *J. Med. Chem.* **1996**, *39*, 4396.

4) Rastelli, G.; Vianello, P.; Barlocco, D.; Costantino, L.; Del Corso, A.; Mura, U. *Bioorg. Med. Chem. Lett.* **1997**, *7*, 1897.

5) Kollman, P. *Chem. Rev.* **1993**, *93*, 2395.

6) Boeseken, J. *Rec. Trav. Chim.* **1939**, *58*, 3.

7) Kaye, I.A.; Metthews, R.S.; Scala, A.A. *J. Chem. Soc.* **1964**, 2816.

8) Bash, P.A.; Singh, U.; Langridge, R.; Kollman, P.A. *Science*, **1987**, *236*, 564.

9) McCammon, J.A. *Science* **1987**, *238*, 486.

10) Jorgensen, W.L.; Briggs, J.M.; *J. Am. Chem. Soc.* **1989**, *11*, 4190.

11) Kuyper, L.F.; Hunter, R.N.; Ashton, D.; Merz Jr., K.M.; Kollman, P.A. *J. Phys. Chem.*, **1991**, *95*, 6661.

12) Miller, J.L.; Kollman, P.A. *J. Phys. Chem.* **1996**, *100*, 8587.

13) Pearlman, D.A.; Case, D.A.; Caldwell, J.W.; Ross, W.S.; Cheatman III, T.E.; Ferguson, D.M.; Seibel, G.L.; Singh, U.C.; Weiner, P.K.; Kollman, P.A., *AMBER 4.1*, University of California, San Francisco, 1995.

14) Cornell, W.D.; Cieplak, P.; Bayly, C.I.; Gould, I.R.; Merz Jr., K.M.; Ferguson, D.M.; Spellmeyer, D.C.; Fox, T.; Caldwell, J.W.; Kollman, P.A. *J. Am. Chem. Soc.*, **1995**, *117*, 5179.

15) van Gunsteren, W.F.; Berendsen, H.J.C *Mol. Phys.* **1977**, *34*, 1311.

16) Ehrig, T.; Bohren, K.M.; Prendergast, F.G.; Gabbay, K.H. *Biochemistry* **1994**, *33*, 7157.

17) Bayly, C.I.; Cieplak, P.; Cornell, W.D.; Kollman, P.A., *J. Phys. Chem.* **1993**, *97*, 10269.

18) Cieplak; P.; Bayly, C.I.; Cornell, W.D.; Kollman, P.A., *J. Comput. Chem.* **1995**, *16*, 1357.

19) Jorgensen, W.L.; Chandrasekhar, J.; Madura, J.D.; Impey, R.W.; Klein, M.L. *J. Chem. Phys.* **1983**, *79*, 926.

20) Cramer, C.J.; Truhlar, D.G. *Science* **1992**, *256*, 213.

21) Cramer, C.J.; Hawkins, G.D.; Lynch, G.C.; Giesen, D.J.; Rossi, I.; Storer, J.W.; Truhlar, D.G.; Liotard, D.A. AMSOL version 5.0, QCPE 606.

22) Cheng, Y.C.; Prusoff, W.H. *Biochem. Pharmacol.* **1973**, *22*, 3099.

23) Checa, A.; Ortiz, A.R.; Pascual-Teresa, B.; Gago, F. *J. Med. Chem.* **1997**, *40*, 4136.